

# Shear Capacity of HPFRC Beams Flexurally Reinforced with Steel and Prestressed GFRP Bars

**F. Soltanzadeh<sup>1</sup>, H. Mazaheripour<sup>2</sup>, J. Barros<sup>3</sup>, J. Sena-Cruz<sup>4</sup>**

<sup>1</sup>ISISE, University of Minho, Guimarães, Portugal, [f.soltanzadeh@civil.uminho.pt](mailto:f.soltanzadeh@civil.uminho.pt)

<sup>2</sup>ISISE, University of Minho, Guimarães, Portugal, [hmp@civil.uminho.pt](mailto:hmp@civil.uminho.pt)

<sup>3</sup>ISISE, University of Minho, Guimarães, Portugal, [barros@civil.uminho.pt](mailto:barros@civil.uminho.pt)

<sup>4</sup>ISISE, University of Minho, Guimarães, Portugal, [jsena@civil.uminho.pt](mailto:jsena@civil.uminho.pt)

**Keywords:** High Performance Fiber Reinforced Concrete; Hybrid Steel/GFRP Flexural Reinforcing System; Shear Failure; Design Codes.

## SUMMARY

*This paper presents the relevant results from an experimental program to assess the shear capacity of high performance fiber reinforced concrete (HPFRC) beams flexurally reinforced with a hybrid system of passive steel and prestressed GFRP longitudinal bars. Three series of two beams with different level of prestressing were tested. The effect of prestressing level on the shear capacity of the beams was the main investigated parameter. The results showed an enhancement of the load carrying capacity, ductility and energy absorption with the increase of the prestress level. Based on the obtained results, the predictive performance of the analytical formulations of CEB-FIP Model Code 2010 and RILEM TC 162-TDF for the shear capacity of FRC beams was assessed. Both formulations seem appropriate for design purposes, but the CEB-FIP formulation predicts more conservative shear capacity. The experimental results demonstrated that the prestressing level has an effect on the shear capacity much higher than the one recommended by the codes.*

## 1. INTRODUCTION

Nowadays, Glass Fiber Reinforced Polymer (GFRP) materials are being used as a competitive alternative for innovative construction systems and for the reinforcement of concrete structures. The major driving force behind this effort is the superior performance of this type of reinforcing system in corrosive environments, non-conductivity and high strength-to-weight ratio [1].

Despite of all these advantages, GFRP has a relatively low modulus of elasticity and brittle tensile failure. Additionally, the bond performance between GFRP bar and concrete is normally lower than conventional steel bars and it strongly depends on the surface treatments of the bar [2, 3].

To improve the ductility and accomplish the serviceability limit state requirements of the GFRP reinforced concrete (RC) beams, it is suggested to include steel bars for the reinforcement of concrete structures [4]. Prestressing GFRP bars can also contribute to overcome the obstacles created by the lower modulus of elasticity, to control the crack width and increase the shear capacity of RC beams.

On the other hand, discrete steel fibers is an interesting reinforcement, mainly for high strength concrete, since they can totally replace steel stirrups without occurring shear failure [5-12]. Using a steel fiber reinforced concrete of high compressive strength and high post-cracking flexural tensile strength, herein designated as high performance fiber reinforced concrete (HPFRC), prefabricated beams not susceptible to corrosion can be developed. In these beams steel stirrups are replaced by steel fibers and the flexural reinforcement is composed by pre-stressed GFRP bars with the minimum acceptable cover thickness [12] and steel bars with a cover thickness that avoids corrosion phenomenon. Since the steel stirrup is the reinforcement that is more susceptible to corrosion due to its

proximity to the exterior surfaces of the beams, replacing it by steel fibers contributes to avoid corrosion problems, which decreases the costs maintenance and increases the structure's durability. In addition to that, the bond between GFRP bars and surrounding concrete may be improved by the presence of the steel fibers [12].

Despite of the extensive research on the behavior of beams without shear reinforcement [13-15], the shear capacity of steel fiber reinforced concrete (SFRC) beams flexurally reinforced with a hybrid system composed of GFRP and steel bars cannot be estimated by using existing results due to the specificities introduced by the presence of the pre-stressed GFRP bars and the use of HPFRC.

The objective of this paper is to assess the shear capacity of HPFRC beams flexurally reinforced with passive steel bars and pre-stressed GFRP. The influence of the pre-stress level applied to the GFRP bars in the behavior of this type of beams is the main investigated parameter. By using the results obtained in the experimental program, the reliability of the analytical formulations proposed by CEB-FIP MC2010 [16] and RILEM TC-162-TDF 2005 [17] for the prediction of the shear capacity of SFRC beams is assessed.

## 2. EXPERIMENTAL PROGRAM

The experimental program is composed of six short-span HPFRC beams reinforced with hybrid prestressed GFRP and passive steel longitudinal bars. The shear capacity of these beams was firstly calculated by means of an analytical formulation recommended in MC2010 for beams without shear reinforcements. Based on the calculated shear capacity, the HPFRC beams were flexurally reinforced with GFRP and steel bar in order to have the shear failure.

### 2.1. Materials

#### 2.1.1. High Performance Fiber Reinforced Concrete (HPFRC)

Table 1 presents the concrete composition used in the present work. Portland cement type I 42.5R was used for preparing the mix. Fly ash and lime stone filler are added to the mix in order to improve the property of the paste. Glenium SKY 617 super plasticizer which is based on second-generation poly carboxylate ether (PCE) polymers is used to provide the suitable flowability. The crushed granite coarse aggregate, river sand, and fine sand, respectively with 12.5 mm, 4.75 mm and 2.35 mm maximum size is included to the aggregate skeleton of the concrete. The concrete is reinforced using 90 kg/m<sup>3</sup> hooked ends steel fibers of 33 mm length ( $l_f$ ), aspect ratio ( $l_f/d_f$ ) of 65 and tensile strength of 1100 MPa. A diameter of 650 μm was obtained in the slump flow test, without occurring segregation. By performing compression tests on five cylindrical specimens of 150 mm diameter and 300 mm high, an average compressive strength of 64.9 MPa [18] and an average Young's modulus of 34.3 GPa were obtained according to the recommendations of [19], with a coefficient of variation of 4% and 2%, respectively. The characteristic value of this HPFRC is 56.9 MPa, which according to the CEB-FIP Model Code [16] is a concrete of C60 strength class.

**Table 1:** Concrete compositions

Mix Design	<i>Cement</i>	<i>Fly ash</i>	<i>Lime stone filler</i>	<i>Water</i>	<i>Super Plasticizer</i>	<i>Fine sand</i>	<i>River Sand</i>	<i>Coarse Agg</i>	<i>Steel Fiber</i>
	<i>kg/m<sup>3</sup></i>	<i>kg/m<sup>3</sup></i>	<i>kg/m<sup>3</sup></i>	<i>Liter/m<sup>3</sup></i>	<i>Liter/m<sup>3</sup></i>	<i>kg/m<sup>3</sup></i>	<i>kg/m<sup>3</sup></i>	<i>kg/m<sup>3</sup></i>	<i>kg/m<sup>3</sup></i>
	462	138	139	208	16	99	697	503	90

To assess the flexural behavior of HPFRC, three prismatic specimens 600×150×150 mm<sup>3</sup> were cast and subjected to the three point bending test according to the recommendations of CEB-FIP MC2010. The Force-CMOD (crack mouth opening displacement) and the Force-Deflection obtained in the notched beam bending tests are plotted in Figures 1a and 1b. Based on the force values for the CMOD<sub>j</sub> (j=1 to 4), the corresponding force values, F<sub>j</sub>, were obtained, and the derived residual flexural tensile strength parameters were determined from the following equation:

$$f_{R,j} = \frac{3F_j L}{2bh_{sp}^2} \quad (1)$$

where  $f_{R,j}$  [N/mm<sup>2</sup>] and  $F_j$  [N] are, respectively, the residual flexural tensile strength and the force corresponding to CMOD=CMOD<sub>j</sub> [mm]. The obtained  $f_{R,j}$ , as well as the limit of proportionality,  $f_{cl,L}^f$  are presented as Table 2.

**Table 2:** Residual flexural tensile strength parameters of the tested Prismatic Specimens (PS)

Specimen ID	Residual tensile strength parameters				$f_{R,3}/f_{R,1}$	$f_{cl,L}^f$
	CMOD1=0.5	CMOD2=1.5	CMOD3=2.5	CMOD4=3.5		
	mm	mm	mm	mm		
	$f_{R,1}$	$f_{R,2}$	$f_{R,3}$	$f_{R,4}$		$f_{cl,L}$
	MPa	MPa	MPa	MPa		kN
PS1	14.24	15.84	15.02	12.83	1.05	8.17
PS2	16.23	18.42	14.91	11.07	0.92	7.97
PS3	14.98	17.28	15.44	14.45	1.03	6.24
Average:	15.15	17.18	15.12	12.78	0.99	7.46
(CoV):	6.66	7.53	1.85	13.24	7.29	14.22

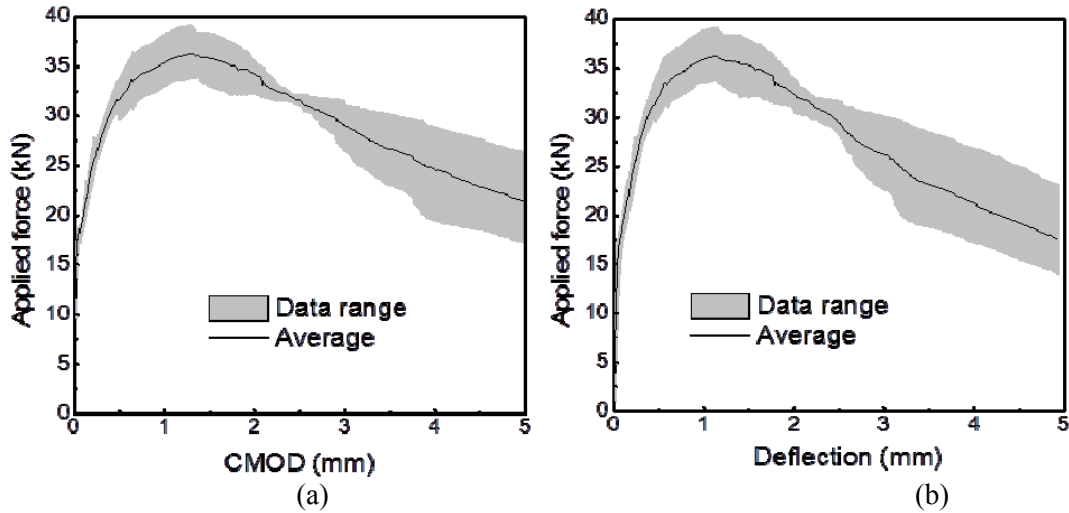


**Figure 1:** Results of the notched beam tests in terms of (a) Force-CMOD and (b) Force-Deflection

### 2.1.2. Reinforcing System of the Beams

Each beam was reinforced longitudinally with three passive steel bars and a GFRP bar, both of 12 mm diameter ( $\phi$ ) and with ribbed-surface. The ribs of the GFRP bar have a constant height of 6% of the bar diameter and a spacing of about 8.5 mm. From tensile tests executed according to the standard ASTM D7205/D7205M-06 [20], an average value of 56 GPa was obtained for a measured diameter of the bar's cross section of 13.0 mm. In contrast with the behavior of the steel bars, the GFRP bar behaves elastically and linearly up to failure. At the supports of the beams, L shape steel bars of 6 mm diameter were applied to avoid premature local failure (Figure 2). Table 3 includes the properties of the reinforcements applied in the present study.

### 2.2. Specimens preparation and test setup

The configuration and test setup of the hybrid steel/GFRP HPFRC beams are shown in Figure 2. The equivalent internal arm of the cross section,  $d_{eq}$ , is 239 mm. The shear span ratio,  $a/d_{eq}$ , is 2.2 in order to promote the occurrence of shear failure. Table 4 indicates the beam's composing of the present experimental program. In the Con series of beams, the GFRP bars were applied without any prestress,

while in series P20 and P30 a prestress level of 20% and 30% of the ultimate tensile capacity of the GFRP bars (1350 MPa) was adopted.

**Table 3:** Mechanical properties of GFRP and steel bars [21]

<i>Type of bar</i>	<i>Diameter</i>	<i>Density</i>	$f_{ty}$	$\epsilon_{ty}$	<i>Young' Modulus</i>	$f_{tu}$	$\epsilon_{tu}$
	<b>mm</b>	<b>gr/cm<sup>3</sup></b>	<b>N/mm<sup>2</sup></b>	<b>%</b>	<b>GPa</b>	<b>N/mm<sup>2</sup></b>	<b>%</b>
GFRP	12 (13.0)	2.23	No yielding	No yielding	67 (56)	1350	7.4
Steel	6	7.85	500	2.3	217	594	45
Steel	12	7.85	490	2.5	196	591	215

Notes:  $f_{ty}$  and  $\epsilon_{ty}$  are the tensile stress and strain at the yielding point:  $f_{tu}$  and  $\epsilon_{tu}$  are the ultimate tensile stress and strain.

**Table 4:** Details of the prepared specimens

<i>Specimen ID</i>	<i>Prestressing level</i>	<i>Prestressing</i>	<i>Loss of stress at the time of testing</i>
	<b>(%)</b>	<b>(MPa)</b>	<b>(%)</b>
B1-Con	Control	-	-
B2-Con	Control	-	-
B1-P20	20	270	5.07
B2-P20	20	270	
B1-P30	30	450	2.32
B2-P30	30	450	

The prestressing procedure was carried out by placing the GFRP bar in the mold and pulling out to obtain the desired levels of prestressing using a coupler hydraulic jack system (see Figure 2). The rate of prestressing was 0.8 kN/min. By measuring the strains recorded in the strain gages installed in the bars (see Figure 3) and taking into account the force value registered in a load cell attached to the actuator, it was verified that when the beams were cast the GFRP bar had the desired prestress level. In all the prestressed beams the prestress was released 3 days after casting. The beams were cured at the average temperature of 23°C and 60% moisture for 7 days. The beams were tested at the age of 28 days. At this age, the loss of prestress was 5.07% and 3.23% for the series P20 and P30, respectively (Table 4).



**Figure 2:** Prestressing system using a coupler hydraulic jack

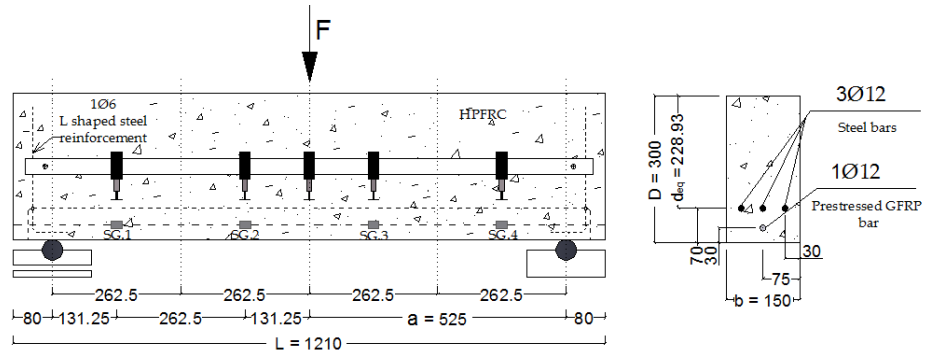


**Figure 3:** Beam configuration and test setup (dimensions in mm)

Deflection of the beams was measured using six Linear Voltage Differential Transducers (LVDTs) disposed according to the arrangement indicated in Figure 3. Another LVDT was also used to control the loading procedure at a displacement rate of 10  $\mu\text{m/s}$  up to the failure of the beams. Four strain gauges (SGs), named as SG1 to SG4, were installed on GFRP surface to measure the strains. The applied load ( $F$ ) was measured using a load cell of  $\pm 700$  kN and  $\pm 0.05\%$  accuracy.

### 2.3 Experimental Results

The average response in terms of force-midspan deflection of the tested series of beams is represented in Figure 4. By increasing the prestress level, the load carrying capacity was increased without affecting significantly the deflection at maximum load. Table 5 resumes the relevant results. The first crack was detected at a load level between 50 to 75 kN in the case of control beams, and 110 to 140 kN in the prestressed beams. Figure 5 shows the crack patterns registered at the failure of the beams. All the beams were failed in shear and the steel bars have yielded before reaching to the ultimate shear capacity.

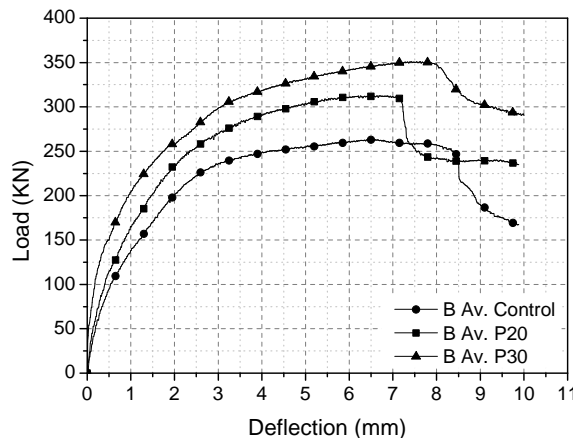


**Figure 4:** Average Load-Deflection relationship at the mid-span for the tested series of beams

Based on the maximum shear load obtained for each beam, it is found that applying a percentage of GFRP bar of 0.25% (ratio between cross-section of GFRP bar and cross-section of concrete) with a prestress level of 20% and 30%, an increase on the shear capacity of, respectively, 19% and 27% was obtained.

Based on the deformation-based approach introduced by Wang and Belarbi [22], in the present study the ductility is defined by the deformability margin between the ultimate stage and the extremity of the linear elastic stage, taking into account the strength effect ( $C_s$ ) as well as the deflection effect ( $C_d$ ).

Based on this definition, the ductility index  $DF$  is expressed as follow:

$$DF = C_s \times C_d \quad (2)$$

where

$$C_s = \frac{P_u}{P_{\delta_1}} \quad (3)$$

$$C_d = \frac{\delta_u}{\delta_1} \quad (4)$$

where  $P_u$  is the load at failure point and  $\delta_u$  is the corresponding deflection at this point.  $P_{\delta_1}$  is the load value at the initiation of the first crack, might be estimated based on the linear elastic equation using Eq. (5).

$$f_{ct}^{cr} = \frac{P_{\delta_1} \cdot L \cdot h}{8I_c} - \sigma_{cp} \quad (5)$$

where  $f_{ct}^{cr}$  is the flexural tensile strength of HPFRC, accepted as the limit of proportionality  $f_{ct,L}^f$ ;  $L$  is the span of the beam,  $h$  and  $I_c$  respectively are the depth and the moment of inertia of the uncracked cross section.  $\sigma_{cp}$  is the average compressive stress acting on the concrete cross section.

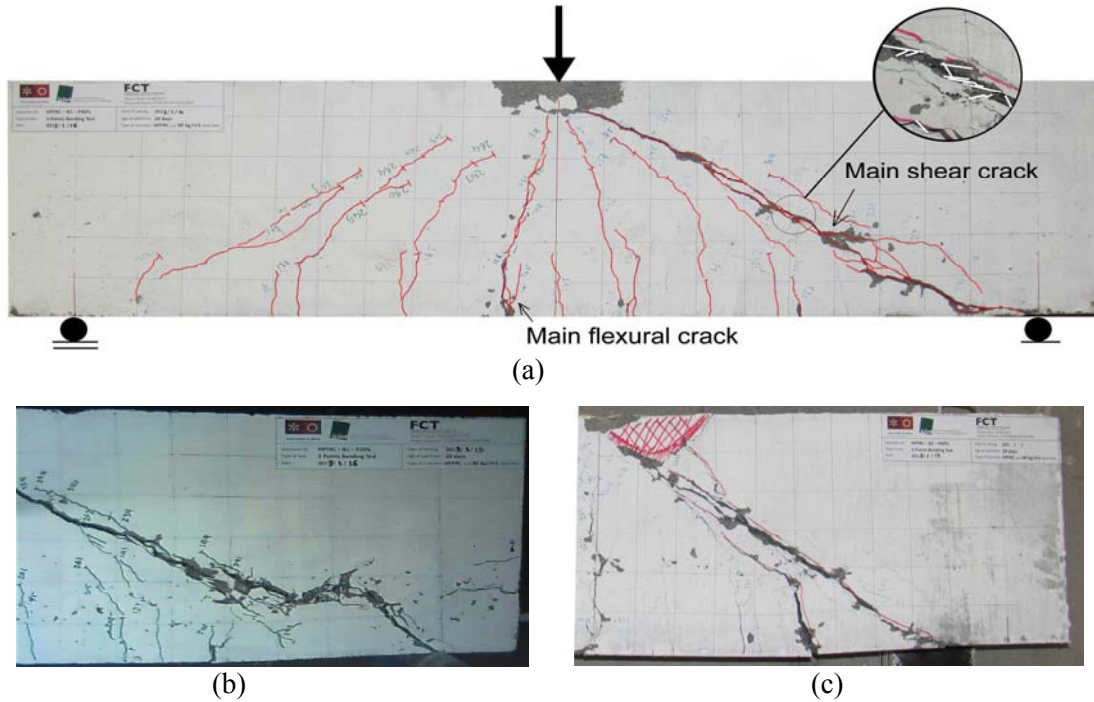


**Figure 5:** Crack pattern of (a) the beam with 30%, (b) 20% prestress and (c) control beam

**Table 5:** Ductility factor and energy absorption of the beams

<i>Specimen ID</i>	<i>Level of prestressing (%)</i>	$P_{\delta_1}$ kN	$P_u$ kN	$\delta_1$ (mm)	$\delta_u$ (mm)	<b>DF</b>	<i>Absorbed Energy (kN.mm)</i>
B <sub>AV</sub> . Con	-	64	263.3	0.26	6.59	104.3	2135.98
B <sub>AV</sub> . P20	20	70	312.8	0.22	6.55	133.0	2458.97
B <sub>AV</sub> . P30	30	73	351.0	0.085	7.62	431.0	3348.08

Table 5 highlights a ductility factor (DF) enhancement by increasing the level of prestress. Consequently, the prestress has also contributed to a significant increase in the energy absorption registered in the prestressed beams when compared to control beams. The energy absorption was computed by measuring the area under the average load-deflection curves up to  $\delta_u$  where  $\delta_u$  is the deflection at maximum load (see Table 5).

### 3. CODE PREDICTIONS

In the present section, the shear capacity of the tested beams is compared with the predictions according to the formulations proposed by CEB-FIP MC2010 [16] and RILEM TC 162-TDF [17]. It is worth noticing that the average values were adopted for the material properties and unit value for the partial safety factor ( $\gamma_c = 1$ ).

### 3.1 CEB-FIP MC2010

According to CEB-FIP MC2010 [16], the shear capacity of the concrete elements  $V_{Rd}$  comprises the shear capacity provided by the Fiber Reinforced Concrete (FRC),  $V_{Rd,F}$ , and by the steel stirrups  $V_{Rd,s}$  (see Eq. 6).

$$V_{Rd} = V_{Rd,F} + V_{Rd,s} \quad (6)$$

where

$$V_{Rd,F} = \left[ \frac{0.18}{\gamma_c} \cdot k \cdot \left[ 100 \cdot \rho_l \cdot \left( 1 + 7.5 \cdot \frac{f_{Ftu,k}}{f_{ck}} \right) f_{ck} \right]^{1/3} + 0.15 \cdot \sigma_{cp} \right] b_w d \quad (7)$$

In this equation,  $d$  is the effective depth of the cross section;  $b_w$  is the width of the cross section and  $\gamma_c$  is the partial safety factor for concrete. In Eq. (6),  $k$  is a factor related to the size effect that can be calculated according to Eq. (8), and  $\rho_l$  is the longitudinal reinforcement ratio determined from Eq. (9), where  $A_{sl}$  is the cross section area of the longitudinal bars.

$$k = 1 + \sqrt{200/d} \leq 2 \quad (8)$$

and

$$\rho_l = A_{sl} / b_w d \quad (9)$$

In Eq. (7),  $f_{ct,k}$  and  $f_{ck}$  are, respectively, the characteristic value of the tensile and compressive strength for the concrete matrix, and  $f_{Ftu,k}$  is the characteristic value of the ultimate residual tensile strength for FRC that is determined from [16]:

$$f_{Ftu}(w_u) = f_{Fts} - \frac{w_u}{2.5} \cdot (f_{Fts} - 0.5 \cdot f_{R3} + 0.2 \cdot f_{R1}) \geq 0; \quad (10)$$

by considering  $w_u = 1.5$  mm and  $f_{Fts}$  equals to  $f_{R3} / 3$  assuming *rigid-plastic model* described in [16]. All the parameters related to the HPFRC can be obtained from the data given in Section 2.1.1 and Table 2.

Table 6 presents shear capacity of the tested beams ( $V_{exp}$ ) and the values estimated according to the formulation proposed by CEB-FIP MC 2010 ( $V_{MC2010}$ ), where average values were adopted for the material properties, and  $\gamma_c = 1$ . It is verified that  $V_{exp} / V_{MC2010}$  has ranged from 1.51 to 1.81, and has increased with the prestressing level.

In the present analysis  $V_{Rd,s}$  was considered to be null.

### 3.2 RILEM Model

According to RILEM guidelines [17], the shear capacity of a RC-SFRC beam is determined from:

$$V_{Rd3} = V_{cd} + V_{fd} + V_{wd} \quad (11)$$

where

$$V_{cd} = \left[ 0.12 k (100 \rho_l \cdot f_{ck})^{1/3} + 0.15 \sigma_{cp} \right] \cdot b_w \cdot d \quad (12)$$

is the concrete contribution, and

$$V_{fd} = 0.7 \cdot k_f \cdot k \cdot \tau_{fd} \cdot b_w \cdot d \quad (13)$$

is the contribution of steel fiber reinforcement. The meaning of the symbols in Eq. (11) was already provided. In Eq. (12), and for the present beams  $k_f = 1$ , while

$$\tau_{fd} = 0.12 f_{Rk,A} \quad (14)$$

**Table 6:** Shear capacity (kN) calculated experimentally and analytically

<i>Specimen ID</i>	$V_{exp}$ (KN)	<i>Average</i> $V_{exp}$ (KN)	$V_{MC\ 2010}^*$ (KN)	$\frac{V_{exp}}{V_{MC\ 2010}}$	$V_{RILEM}^{**}$ (KN)	$\frac{V_{exp}}{V_{RILEM}}$	$\frac{V_{RILEM}}{V_{MC\ 2010}}$
B1-Con	127.52	133.5	88.3	1.51	156.3	0.85	1.80
B2-Con	139.48						
B1-P20	149.96	159.1	91.8	1.73	159.8	0.99	1.74
B2-P20	168.23						
B1-P30	162.09	169.3	93.5	1.81	161.6	1.05	1.73
B2-P30	176.49						

\* from Eq. (3); \*\* form Eq. (8)

In the present analysis  $V_{wd}$  was considered to be null. Since, the average values were taken into account while the characteristic values appeared in the formula, 0.12 was replaced by  $0.18/\gamma_c$  in Eq. (7) and (12), where  $\gamma_c = 1$ .

The calculated shear capacity using RILEM proposal can be found in Table 6. The ratio of the shear capacity obtained experimentally to that of calculated using this guideline  $V_{exp}/V_{RILEM}$  increased by increasing the level of prestressing from 0.85 to 1.05.

A significant difference was observed between the results calculated using both of the introduced guidelines.

#### 4. DISCUSSION

Comparing Eq. (7) recommended by MC 2010 with Eq. (12) proposed by RILEM guideline, it can be concluded that the included effect of fibers in Eq. (7) is only dependent on  $f_{Ftuk}/f_{ctk}$ . Thus by calculating the shear capacity of a plain concrete using MC 2010, the introduced term ( $f_{Ftuk}/f_{ctk}$ ) will be null. The shear capacity was calculated using MC 2010 formula for the plain concrete only. By subtracting this value from the shear capacity calculated for the fiber reinforced concrete, the effect of fiber contribution was obtained. This effect was compared with that of calculated using RILEM guideline ( $V_{fd}$ ) thereafter. Figure 6a shows the magnitude of the shear capacity provided by the fibers contribution “ $V_{fd}$ ” using both of the provisions. The estimated value of  $V_{fd}$  by RILEM is significantly (almost 2.7 times) higher than that of calculated by MC2010.

Additionally the effect of prestressing on the improving trend of shear capacity, which is related to the term  $0.15 \sigma_{cp} b_w d$ , was the same using both guidelines. However, this improvement was not at the same rate of improving trend of shear capacity obtained experimentally (see Figure 6b). About 21% improvement was achieved in the tests by increasing the level of prestress, while the shear capacity of HPFRC increased 9.6% only according to both guidelines. Based on the experimental achievement, it seems that the favorable effect of prestressing on the shear capacity is not being well quantified in CEB-FIP MC2010 and RILEM. This shows the requirement of extra attention for including the effects of prestressing on the shear capacity with more accuracy in the formula.

The total shear capacity “ $V_{Rd}$ ” calculated by RILEM is closer to the experimental results, which is due to the high estimated  $V_{fd}$ . On the contrary, MC2010 has estimated lower values for the shear capacity provided by the fiber contribution. Since a constant content of steel fiber was adopted in this experimental program, the accuracy on the evaluation of the fiber contribution to the shear capacity cannot be concluded.



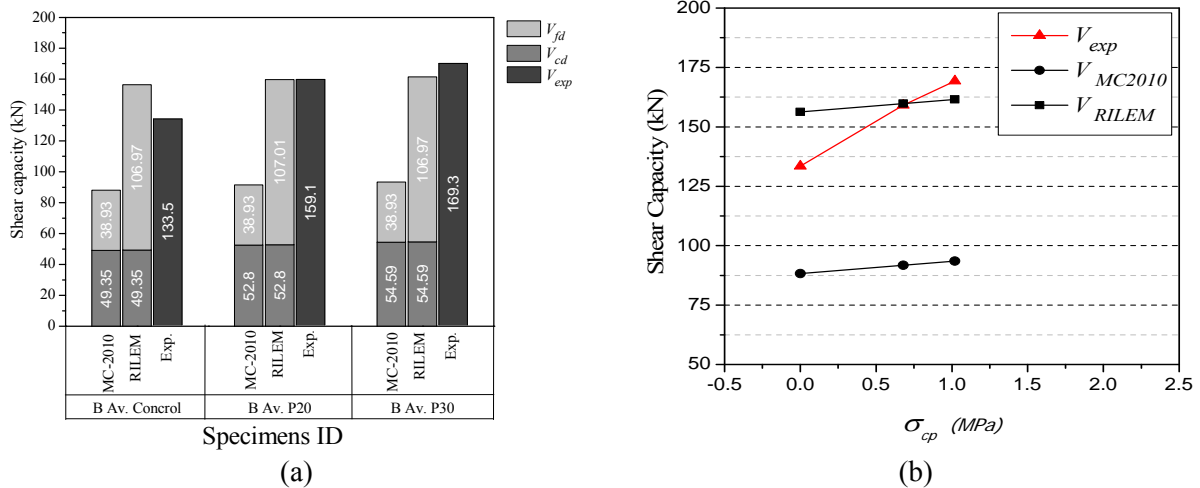


**Figure 6:** (a) Comparison of the effect of  $V_{fd}$  and  $V_{cd}$  (b) Shear capacity vs.  $\sigma_{cp}$ ;

## 5. CONCLUSIONS

Three series of short span beams with different level of prestressing were tested under three-point bending test to compare the experimental shear capacity with the analytical models recommended by fib MC2010 proposal and RILEM TC 162-TDF guideline. A summary of remarks can be drawn as follow:

- Including the prestressed GFRP bar into the hybrid steel/GFRP flexural reinforcing system in the present study, resulted a significant improvement of the shear capacity compared to the beams with the passive GFRP bars. Consequently a significant increase of the energy absorption is found by prestressing the beams.
- In all the beams, it was observed that the ductility factor enhanced significantly by increasing the level of prestressing.
- The shear capacity obtained experimentally increased almost 21% by increasing the level of prestressing up to 30% of GFRP ultimate tensile strength while this value was analytically predicted as 9.6% only. This shows the requirement of extra attention for including the effects of prestressing on the shear capacity with more accuracy in the formula.
- Both formulations seem appropriate for design purposes. However, the effect of prestressing should be more taken in to account in the related formula.
- To have the better judgment about the effects of fiber contribution in the estimation of shear capacity, testing specimens with different fiber volume fraction is required.

## ACKNOWLEDGEMENTS

The research in this paper is part of the project “DURCOST - Innovation in reinforcing systems for sustainable pre-fabricated structures of higher durability and enhanced structural performance” with reference number of PTDC/ECM/105700/2008, supported by FCT. The authors also thank the collaboration of the following companies: Sireg and Schoeck for providing the GFRP bars, Casais to manufacture the moulds, Maccaferri for supplying the steel fibres, Secil/Unibetão for providing the Cement, SIKA for supplying the superplasticizers; CiviTest for the production of SFRSCC specimens. The first and the second authors acknowledge the research grant in the ambit of this project and from the PhD program from FCT (SFRH/BD/77409/2011), respectively.

## REFERENCE

- [1] Sharbatdar M. K., (2008), “Monotonic and cyclic loading of new FRP reinforced concrete cantilever beams,” International Journal of Civil Engineering. Vol. 6, No. 1, pp 58-71.
- [2] Achilides Z, Pilakoutas K., (2004), Bond behavior of fiber reinforced polymer bars under direct pullout condition,” J Compos Constr, 8, (2), pp 173-181

- [3] Al-Mahmoud F, Castel A, Francois R, Tourneur C. (2007), "Effect of surface pre-conditioning on bond of carbon fiber reinforced polymer rods to concrete," *Cem Concrete Composit Journal*, 29, (9), pp 677-689.
- [4] Lau D. and Pam H. J., (2010), "Experimental study of hybrid FRP reinforced concrete beams," *Journal of Engineering Structures*, 32, pp 3857–3865.
- [5] Kwak Y. K., Eberhard M. O., Kim W. S., Kim J., (2002), "Shear strength of steel fiber reinforced concrete beams without stirrups," *ACI Structural Journal*, Title No. 99-S55, pp 530\_538.
- [6] Hisabe N., Yoshitake I., Tanaka H., and Hamada S., (2006), "Mechanical behaviour of fiber reinforced concrete element subjected to pure shearing stress," *International RILEM workshop on High performance fiber reinforced cementations composites in structural applications*, RILEM PUBLICATION SARL, pp 375-381.
- [7] Sagaseta J. and Vollum R. L., (2011), "Influence of aggregate fracture on shear transfer through cracks in reinforced concrete," *Magazine of Concrete Reinforced*, Vol. 63, Issue 2, pp 119-137.
- [8] Zdenek P. B., Prat P. C. and Tabbara M. R., (1990), "Antiplane Shear Failure Tests (Mode II)," *ACI Material Journal*, No. 87-M7, pp 12-19.
- [9] Banzant Z. P. and Pfeiffer P. A., (1986), "Shear fracture tests of concrete," *Materiaux et Constructions*, Vol. 19, No. 110, pp 111-121.
- [10] Vall M. and Buyukozturk O., (1993), "Behaviour of fiber reinforced high-strength concrete under direct shear," *ACI Material Journal*, Title No. 90-M13, pp 122-133.
- [11] Minelli, F., (2005), "Plain and fiber reinforced concrete beams under shear loading: structural behaviour and design applications," PhD thesis, Department of Civil Engineering, University of Brescia, Starrylink Editrice, Brescia, Italy, 429 .
- [12] Mazaheripour H, Barros J, Sen-Cruz J, Pepe M, Martinelli E.(2013), "Experimental study on bond performance of GFRP bars in self-compacting steel fiber reinforced concrete" *J.. Compos Struct*, 95, pp202-12.
- [13] Banzant Z.P. and Yu Q., (2005), "Designing against size effect on shear strength of reinforced concrete beams without stirrups," *Journal of Structural Engineering*, V131, Issue 12, pp 1877-1885.
- [14] Lingemann J., Sauer J., and Zilch K., (2010), "Shear capacity of steel fiber reinforced concrete beams with stirrups," *3rd fib International Congress*.
- [15] Ding Y., Youb Z., Jalali S., (2011), "The composite effect of steel fibers and stirrups on the shear behaviour of beams using self-consolidating concrete," *Journal of Engineering Structures* 33, pp 107–117.
- [16] CEB-FIP. *Model Code 2010*: Final Draft. Model Code prepared by Special Activity Group 5, Lausanne, September 2011.
- [17] Vandewalle, L. et al., "Test and design methods for steel fibre reinforced concrete - Final Recommendation", *Materials and Structures*, 35(253), 579-582, Nov. 2002.
- [18] ASTM C39 / C39M - 12a Standard Test Method for Compressive Strength of Cylindrical Concrete Specimens.
- [19] E365 (1993). "Hardened Concrete - Determination of the modulus of elasticity of concrete in compression." National Laboratory for Civil Engineering Specification, 2 pp (in portuguese).
- [20] ASTM D7205/D7205M-06. Standard Test Method for Tensile Properties of Fiber Reinforced Polymer Matrix Composite Bars. ASTM International, US, 2006.
- [21] Dalfre G., (2013), "Flexural and shear strengthening of RC elements," Ph.D Thesis, University of Minho, School of Engineering, Dept. of Civil Engineering, Guimarães, Portugal.
- [22] Wang H., Belarbi A , (2011), "Ductility characteristics of fiber-reinforced-concrete beams reinforced with FRP rebars," *Construction and Building Materials* 25 pp 2391–2401